

A Model for the Lipid Pretransition: Coupling of Ripple Formation with the Chain-Melting Transition

Thomas Heimburg

Max-Planck Institut für biophysikalische Chemie, 37070 Göttingen, Germany

ABSTRACT Below the thermotropic chain-melting transition, lipid membrane c_p traces display a transition of low enthalpy called the lipid pretransition. It is linked to the formation of periodic membrane ripples. In the literature, these two transitions are usually regarded as independent events. Here, we present a model that is based on the assumption that both pretransition and main transition are caused by the same physical effect, namely chain melting. The splitting of the melting process into two peaks is found to be a consequence of the coupling of structural changes and chain-melting events. On the basis of this concept, we performed Monte Carlo simulations using two coupled monolayer lattices. In this calculation, ripples are considered to be one-dimensional defects of fluid lipid molecules. Because lipids change their area by $\sim 24\%$ upon melting, line defects are the only ones that are topologically possible in a triangular lattice. The formation of a fluid line defect on one monolayer leads to a local bending of the membrane. Geometric constraints result in the formation of periodic patterns of gel and fluid domains. This model, for the first time, is able to predict heat capacity profiles, which are comparable to the experimental c_p traces that we obtained using calorimetry. The basic assumptions are in agreement with a large number of experimental observations.

INTRODUCTION

The lipid pretransition is a low enthalpy transition below the chain-melting transition of lipid membranes (Rand et al., 1975; Suurkuusk et al., 1976). It is linked to the formation of periodic ripples on the membrane surface, usually with periods in the range of 100–300 Å, depending on the lipid (Janiak et al., 1976). In some systems, ripple periods up to 1000 Å were found (Brown et al., 1995; Meyer et al., 1996). In the presence of cholesterol, the ripple spacing may become very large (Mortensen, 1988). The range of ripple phase stability spans from the pretransition up to the main transition. Below the pretransition and above the main transition, the membrane surface is planar and the ripples disappear.

The pretransition is considerably less cooperative than the main transition. Its half width is in the range of 1–2°, whereas the main transition has a half width of $\sim 0.05^\circ$ (in DPPC multilayers [Heimburg, 1998]). The temperature interval between pre- and main transition apparently is chain-length dependent. In phosphatidylcholines, it decreases from $\sim 10^\circ$ for DMPC, to 7° for DPPC, 3.1° for DSPC, and

1.2° for the analogue with C_{20} -carbon chains (Jørgensen, 1995). For longer chains, the pretransition disappears (or merges with the main transition).

The pretransition seems to depend on the vesicular state of the lipids. Multilayers display a pretransition, which is clearly distinguishable from the main chain-melting transition. The pretransition, however, can also be found in unilamellar systems (Lichtenberg et al., 1984; Meyer, 1996) where it is broader and less separated from the main transition (Heimburg, 1998). In unilamellar systems, the heat capacity in between the two transitions is found to be above the baseline level. Both transitions seem to represent one continuous event. Furthermore, a pretransition event has been found in asymmetric unilamellar bilayers (Czajkowsky et al., 1995).

The occurrence of the pretransition is dependent on the lipid headgroup. Phosphatidylethanolamines (McIntosh, 1980; Kodama and Miyata, 1996) and glucolipids (Hinz et al., 1985) do not display a pretransition, whereas it is clearly visible in the c_p -traces of phosphatidylcholines and phosphatidylglycerols (Rand et al., 1975). The detection of the pretransition is sensitive to the addition of various biomolecules. Cholesterol affects the ripple periodicity and lowers the pretransition temperature in DMPC (Mortensen et al., 1988; Matuoka et al., 1994). The pretransition is abolished upon the addition of gramicidin S (Prenner et al., 1999), cannabinoids (Mavromoustakos, 1996), sphingosine (Koiv et al., 1993), ursodeoxycholate (Tomoaia-Cotisel and Levin, 1997), various anesthetics (Engelke et al., 1997), and ceramides (Holopainen et al., 1997). There are indications that the absence of the pretransition in DPPC-membranes containing anesthetic steroids may be the consequence of an extreme broadening such that it is not evident in heat capacity (c_p)-traces but is visible by other means (Mavromoustakos et al., 1997).

Received for publication 10 September 1999 and in final form 14 December 1999.

Address reprint requests to Dr. T. Heimburg, Membrane Thermodynamics Group (AG 012), Max-Planck-Institut für biophysikalische Chemie, 37070 Göttingen, Germany. Tel.: +49-551-201-1412; Fax: +49-551-201-1501; E-mail: theimbu@gwdg.de; Web Site: <http://www.gwdg.de/~theimbu>

Abbreviations used: c_p , Excess heat capacity; DMPC, 1,2-dimyristoyl-*sn*-glycero-3-phosphatidylcholine; DMPG, 1,2-dimyristoyl-*sn*-glycero-3-phosphatidylglycerol; DPPC, 1,2-dipalmitoyl-*sn*-glycero-3-phosphatidylcholine; DSPC, 1,2-distearoyl-*sn*-glycero-3-phosphatidylcholine; DSC, differential scanning calorimetry; ESR, electron spin resonance; NMR, nuclear magnetic resonance; FTIR, Fourier transform infrared spectroscopy.

© 2000 by the Biophysical Society

0006-3495/00/03/1154/12 \$2.00

The formation of ripples is dependent on hydration and does not occur in dehydrated lipid membranes. The ripple phase seems to be better hydrated than the planar membrane phases (Inoko and Mitsui, 1978; Janiak et al., 1979; Doniach, 1979; Parsegian, 1983; Cevc, 1991; Scott and McCullough, 1993; Bartucci et al., 1996; Krasnowska et al., 1998; Le Bihan and Pezolet, 1998). Vice versa, the formation of the ripple phase results in an osmotic stress (Perkins et al., 1997).

X-ray crystallography indicates that lipids are packed into a triangular lattice in both the gel state and the ripple phase, whereas it is disordered in the fluid L_α phase (Janiak et al., 1979). This result is supported by atomic force microscopy experiments (Hui et al., 1995). The lipid chains are tilted in the gel state of phosphatidylcholine membranes but are not tilted in the gel state of phosphatidylethanolamine (McIntosh, 1980), suggesting that the tilt may be linked to the formation of the ripple phase.

In the pretransition, most or all thermodynamic variables change, including enthalpy (e.g., Rand et al., 1975), volume (Nagle and Wilkinson, 1978), area (Evans and Kwok, 1982), and chain order parameter (Heimburg et al., 1992; see Fig. 1). Spectral changes in the pretransition can be seen in fluorescence data (Binder and Dittes, 1987; Epps et al., 1997; Krasnowska et al., 1998), ESR (Tsuchida and Hatta, 1988; Heimburg et al., 1992), and infrared experiments (Le

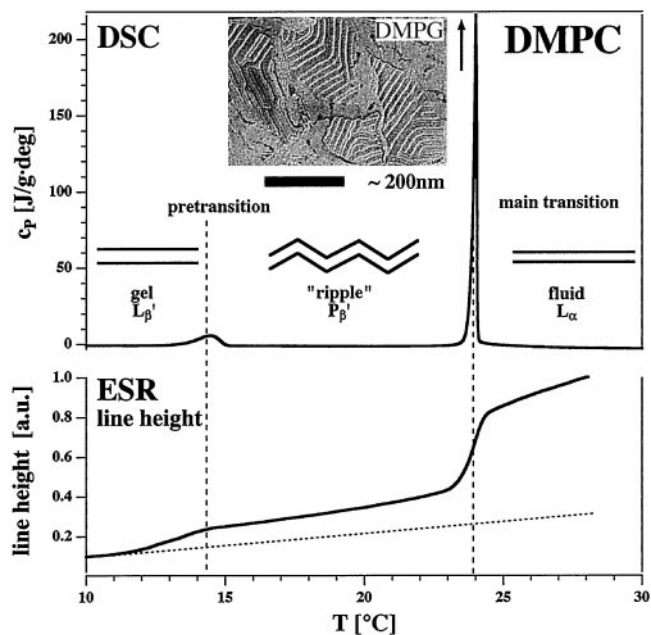


FIGURE 1 Melting profiles of DMPC multilamellar vesicles. *Top*: DSC trace. *Bottom*: Spectral line height of electron spin resonance spectra, using a 5-DMG spin label (adapted from Heimburg et al., 1992). The spectral line height is inversely related to an order parameter. Thus, the ESR results indicate a reduction in order of both pre- and main transition. The insert shows a freeze fracture picture electron micrograph of DMPG vesicles in the ripple phase region (from Schneider et al., 1999). Ripple periods are ~ 280 Å. 120° angles between ripples of different orientation are found.

Bihan and Pezolet, 1998). In freeze fracture electron microscopy and atomic force microscopy, the ripples can be directly visualized (Sackmann, 1995; Czajkowsky et al., 1995; Meyer, 1996; Meyer et al., 1996).

The ripples introduced above the pretransition seem to display both symmetric and asymmetric cross-sections (Woodward and Zasadzinski, 1996; Rappolt and Rapp, 1996; Cunningham et al., 1998; Bota and Kriechbaum, 1998), depending on sample history. It is not clear whether they are in thermal equilibrium. This is further complicated by the fact that the pretransition is very slow (Lentz et al., 1978; Lichtenberg et al., 1984).

The models in the literature are mainly grouped into two classes. Mean field or Landau models use the interplay of the elastic constants (Doniach, 1979; Lubensky and MacKintosh, 1993) and statistical thermodynamics models using vertical degrees of freedom, or tilt angles (Georgallas and Zuckermann, 1986; Scott and Pearce, 1989; McCullough and Scott, 1990; Scott and McCullough, 1991, 1993). Scott and McCullough (1993) reviewed other models, which use the variation of the bilayer thickness. One should mention an interesting paper by Marder et al. (1984) following an idea comparable to our model outlined below. Here a mean field model has been used, coupling membrane curvature to periodic variations of gel- and fluid-rich regions close to the chain-melting regime. A similar idea has been expressed by Leibler and Andelman (1987), who used a coupling of hydrocarbon state with membrane curvature to rationalize the stability of membrane undulations. Although these models may, in part, explain the existence of membrane ripples, they are not satisfactory because they fall short of explaining the pretransition or being able to determine the heat capacity profile of this transition. Furthermore, they do not predict the experimentally observed changes in thermodynamic observables such as excess heat, volume, or area, and they usually make no connection between the pretransition and the main transition. Therefore, one has to conclude that the phenomenon of the pretransition is still not well understood.

The microscopic model presented here differs from all recent models because it considers the transition behavior of individual lipid molecules in two coupled monolayers in a statistical thermodynamic manner. It is assumed that the pretransition is linked to the melting of the lipid chains and that the membrane ripples consist of fluid lipid line defects. By necessity, the pre- and main transitions are coupled in this model. The changes of the thermodynamic observables are a natural result of the calculation. Furthermore, the model allows us to calculate heat capacity profiles that are comparable to experimentally observed heat capacity traces.

MATERIALS AND METHODS

Dipalmitoyl phosphatidylcholine was purchased from Avanti Polar Lipids (Birmingham, AL) and used without further purification. Heat capacities

were recorded on an MC2-calorimeter and a VP-calorimeter from Microcal, Inc. (Northampton, MA) at scan rates of 5°/h and 1°/h. Extruded vesicles were made using a Lipofast extruder (Avestin Inc., Ottawa, Canada) using a polycarbonate filter with pore sizes of 100 nm.

THEORY

Lipid molecules in the gel state are organized in a solid ordered state—usually on a triangular lattice (Janiak et al., 1979; Hui et al., 1995). At the melting transition, the crystalline order is lost and the lipid chains become fluid disordered.

Lipids increase their area in the transition regime by about 24% (for DPPC: Heimburg, 1998). In the literature, this melting process has been modeled by different models, using from two lipid conformational states (Sugar et al., 1994; Heimburg and Biltonen, 1996) to ten lipid conformational states (Pink et al., 1980; Zhang et al., 1992a; Zhang et al., 1993). The strong cooperativity of the transition is modeled by nearest neighbor interactions. In any of those models, lipid domains of different states are formed during the melting process.

Let us assume that the lipid lattice is triangular with three principal axes. The area increase during the melting process disrupts the lattice order if individual lipids melt independently (Fig. 2). Such an event shall be called a point defect. However, if local point defects arrange themselves linearly along a lattice direction, the resulting line defect does not disrupt the crystal order (Fig. 2). We conclude, therefore, that line defects must be energetically favored over uncorrelated point defects. In the following, we will approximate

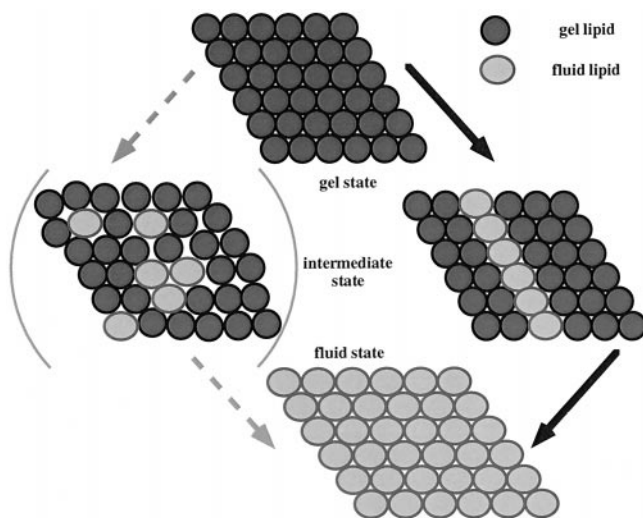


FIGURE 2 Schematic view on a triangular lattice during the melting process. Gel and fluid lipids have different cross-sectional areas. *Top*: All lipids are in the gel state placed on an undistorted lattice. *Center left*: some fluid lipids are randomly arranged in a gel matrix, resulting in lattice distortion. *Center right*: the same number of fluid lipids is arranged in a line defect, which is possible without lattice distortion. *Bottom*: All lipids are in the fluid state, and are situated on an undistorted lattice.

the melting process of a monolayer by allowing only line defects and neglecting individual point defects. This approximation reduces a model calculation of monolayer melting to a one-dimensional problem. In the triangular lattice, there are three possible easy planes, corresponding to the three principal crystal axes that display 120° angles. Interestingly these angles are often seen in electron micrographs showing the relative arrangements of the ripples (e.g., Meyer, 1996; Fig. 1, *insert*).

Let us further assume that a bilayer is constructed from two monolayers with opposing lattice sites. Because of the area increase of the lipids, a close contact of two monolayers creates a strong correlation on the arrangement of defects in both monolayers. This topological constraint is usually neglected in membrane models, although intermonolayer coupling has been discussed before (Zhang et al., 1992b; Hansen et al., 1998). Actually, the only defects that are consistent with maintaining triangular order on both monolayers are line defects that propagate along the same principal axis in both monolayers. Thus, in the following, we will assume that fluid lipid line defects are aligned in both monolayers and we treat the defect-formation process of the lipid bilayer as a one-dimensional problem of two coupled monolayers.

The assumptions outlined above are based on the formation of line defects on two opposing monolayers with triangular lattice packing. Clearly, the occurrence of a line defect in one monolayer leads to an asymmetry of area across the bilayer and, as a result, to a local curvature that is a function of the local area difference (Fig. 3). Assuming, for DPPC, an area change from $\sim 50 \text{ \AA}^2$ to 60 \AA^2 and a

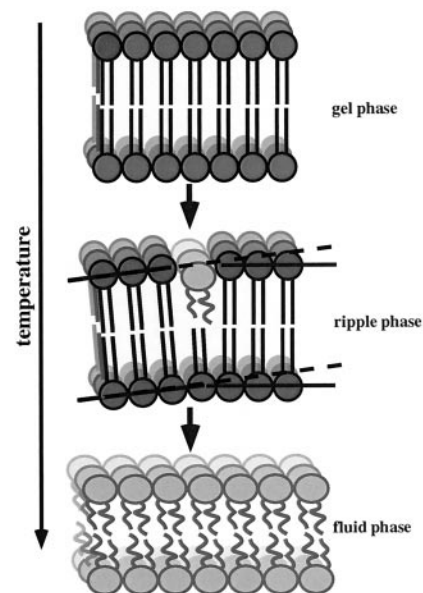


FIGURE 3 Schematic drawing of two coupled lipid monolayers in the gel state with a fluid lipid line defect on one side. The consequence of the area asymmetry is a local bending.

membrane thickness of 47 Å (Heimburg, 1998), one obtains a local radius of curvature of ~ 200 Å. Our model will be based on the assumption that this local curvature—caused by an asymmetry of fluid lipid line defects—is the origin of ripple formation. In the Discussion section, it will be shown that many experimental facts justify this assumption.

In the following section, we outline a simple model that attempts to combine the experimental results described above with the concept of fluid lipid line defects. This model is basically a one-dimensional Ising (or Doniach) model with two coupled monolayers. The Hamiltonian of the two coupled monolayers is composed of several terms. The first term, H_{chain} , is just the sum of the chain enthalpies of all lipid molecules from the two monolayers A and B,

$$H_{\text{chain}} = m \cdot \Delta H \cdot \sum_i (\sigma_i^A + \sigma_i^B), \quad (1)$$

where $\sigma_i^{A,B} = 1$ for fluid lipids in layer A or B, $\sigma_i^{A,B} = 0$ for gel lipids in layer A or B, m is the number of lipids per line defect, and i is the lipid index along the one-dimensional lattice.

Lattice models require a term to introduce cooperativity. This is usually done by the introduction of an interaction term between gel and fluid lipids (unlike nearest neighbors) (e.g., Sugar et al., 1994). The enthalpy contribution H_{NN} is thus the sum of all unlike nearest neighbor interactions on both monolayers A and B with an individual value ω_{gf} (Fig. 4 a):

$$H_{\text{NN}} = m \cdot \omega_{\text{gf}} \cdot \left[\sum_i \left| \sigma_i^A - \sigma_{i-1}^A \right| + \sum_i \left| \sigma_i^B - \sigma_{i-1}^B \right| \right]. \quad (2)$$

When a membrane segment is curved, unlike nearest neighbors possess a different lipid environment depending on whether they are located on the inner or on the outer monolayer (Fig. 4 b). This implies that unlike nearest neighbor interactions may be different in a gel-like than in a fluid-like environment because, in the first case, gel–fluid contacts are located on the outer monolayer and, in the latter case, on the inner monolayer, and are thus differently exposed to solvent. We take this into account by assuming that the nearest neighbor interaction is slightly different on the inner than on the outer monolayer. This has been implemented by introducing a (solvent-dependent) term w_{solv} such that the unlike nearest neighbor interactions on the outer layer are given by $\omega_{\text{gf}} + \omega_{\text{solv}}$, and, on the inner layer, they are given by $\omega_{\text{gf}} - \omega_{\text{solv}}$. The overall solvent-dependent term is defined to be the sum over all local gel–fluid asymmetries of the membrane segment,

$$H_{\text{solv}} = m \cdot \omega_{\text{solv}} \cdot \sum_i \delta_i^{\text{solv}}, \quad (3)$$

with

$$\delta_i^{\text{solv}} = +1 \quad \text{if} \quad \sigma_{i-1}^A + \sigma_{i-1}^B + \sigma_i^A + \sigma_i^B = 1,$$

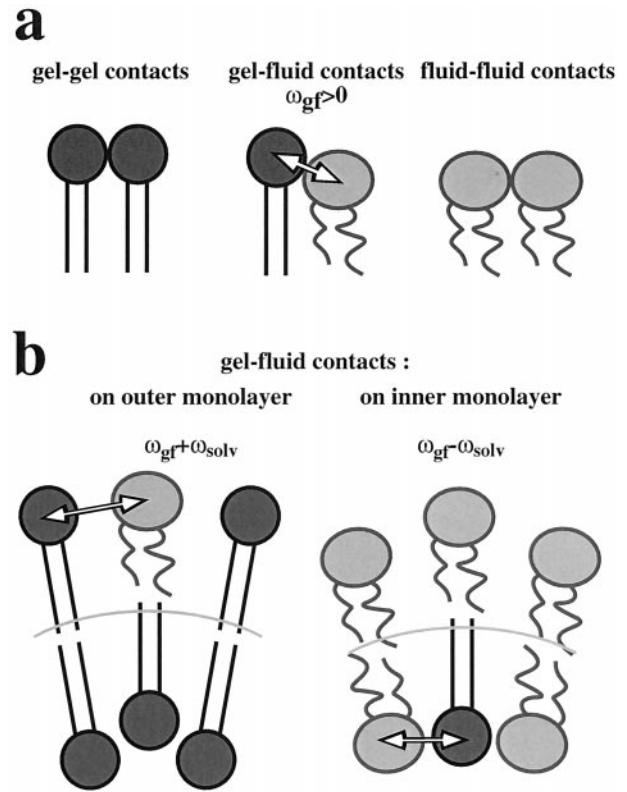


FIGURE 4 Schematic drawing of (a) nearest neighbor lipid–lipid interactions and (b) the interaction of line defects with water.

$$\delta_i^{\text{solv}} = -1 \quad \text{if} \quad \sigma_{i-1}^A + \sigma_{i-1}^B + \sigma_i^A + \sigma_i^B = 3,$$

$$\delta_i^{\text{solv}} = 0 \quad \text{else.}$$

The introduction of a local curvature leads to the interesting problem of whether it is compatible with the overall vesicular topology. Clearly, in a closed vesicle, the local curvatures, if integrated over the whole vesicle, have to maintain the closed topology of the membrane. This leads to the necessity that, on both sides of the membrane, one finds about the same number of line defects. Locally, however, the distribution of line defects is not necessarily homogeneous and may allow for local curvatures. Curvature fluctuations may even lead to changes in shape. In multilayers, the topological constraints are much stronger, because each membrane segment is encaged by adjacent bilayers (Fig. 5 a), such that local curvature fluctuations are hindered (Helfrich, 1978). Macroscopic changes in shape or macroscopic curvature changes are inhibited. Within the limits given by the interbilayer distance, the number of line defects on both monolayers is locally constrained. One may envision the local constraint by the restriction of curvature fluctuations between two hard walls. As shown in Fig. 5 b, this automatically introduces a correlation length, which, in the framework of this model, is linked to the formation of periodic membrane ripples.

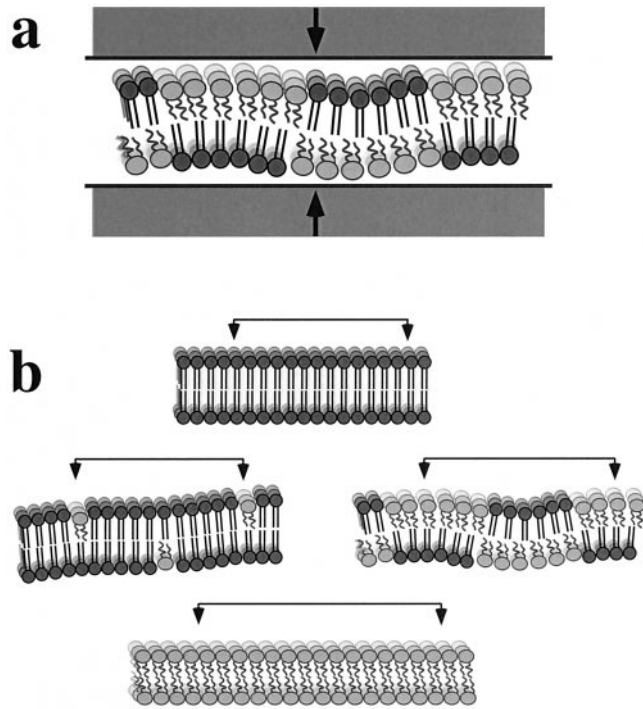


FIGURE 5 (a) Schematic drawing of a lipid bilayer located between two hard walls. In this situation, the number of fluid lipid line defects must be equal in both monolayers to minimize the potential free energy superimposed by geometrical boundary conditions. (b) Periodic solutions are favored if line defects form domains.

We will now phenomenologically introduce a harmonic potential that depends on the difference of line defects within a given correlation length of $2 \cdot l + 1$ line defects around a lipid line defect at site i :

$$H_{\text{geom}} = m \cdot \alpha \cdot \sum_i \left(\sum_{i-l}^{i+l} (\sigma_i^A - \sigma_i^B) \right)^2. \quad (4)$$

This term creates the ripple periodicity. It is constructed such that, in an interval of $i - 1$ to $i + 1$ around the lattice site of index i , a configuration with an equal number of fluid line defects on both sites is energetically favored. An asymmetry of defects is given an energy penalty proportional to the square of the difference of the number of defects. The constant α of this harmonic potential defines the strength of the potential and is assumed to have a larger value for multilayers than for unilamellar systems. It will be shown below that such a potential in the Hamiltonian favors periodic solutions with a period of $(2l + 1)$ lattice sites. The correlation length $2l + 1$ has to be chosen such that it corresponds to experimentally observed ripple spacings. Taking a lipid diameter to be 7 \AA , $l = 20$ corresponds to a ripple spacing of roughly 300 \AA , a value found in DMPG membranes. The overall Hamiltonian energy is the sum of

the four terms introduced above,

$$H = (H_{\text{chain}} + H_{\text{NN}} + H_{\text{solv}} + H_{\text{geom}}). \quad (5)$$

The distribution of states for a given temperature is explored with a Monte Carlo simulation based on a Metropolis algorithm (Metropolis et al., 1953). The bilayer matrix is constructed to consist of two coupled one-dimensional layers, A and B, with periodic boundary conditions. Each point on the lattice corresponds to a line of m gel or fluid lipids. A lattice point on either side of the bilayer is chosen randomly. For this lipid, the decision whether a lipid will be gel or fluid in the next step is taken by calculating an equilibrium constant for this lipid,

$$K_i^{\text{A,B}} = \exp\left(-\frac{\mathcal{A}^{\text{A,B}}}{RT}\right) \quad (6)$$

where

$$\begin{aligned} \mathcal{A}^{\text{A,B}} = & m \cdot [(\Delta H - T \cdot \Delta S) + (\Delta n_{\text{gf},i-1}^{\text{A,B}} + \Delta n_{\text{gf},i+1}^{\text{A,B}})] \cdot \omega_{\text{gf}} \\ & + (\Delta n_{\text{solv},i-1}^{\text{A,B}} + \Delta n_{\text{solv},i+1}^{\text{A,B}}) \cdot \omega_{\text{solv}} + \alpha \cdot P^{\text{A,B}}(i), \end{aligned}$$

with

$$\Delta n_{\text{gf},i-1}^{\text{A,B}} = 1 \quad \text{if} \quad \sigma_{i-1}^{\text{A,B}} = 0;$$

$$\Delta n_{\text{gf},i-1}^{\text{A,B}} = -1 \quad \text{otherwise};$$

$$\Delta n_{\text{gf},i+1}^{\text{A,B}} = 1 \quad \text{if} \quad \sigma_{i+1}^{\text{A,B}} = 0;$$

$$\Delta n_{\text{gf},i+1}^{\text{A,B}} = -1 \quad \text{otherwise};$$

$$\Delta n_{\text{solv},i-1}^{\text{A,B}} = +1 \quad \text{if} \quad \sigma_{i-1}^{\text{A,B}} + \sigma_{i-1}^{\text{B,A}} + \sigma_i^{\text{B,A}} = 0 \text{ or } 3;$$

$$\Delta n_{\text{solv},i-1}^{\text{A,B}} = -1 \quad \text{otherwise};$$

$$\Delta n_{\text{solv},i+1}^{\text{A,B}} = +1 \quad \text{if} \quad \sigma_{i+1}^{\text{A,B}} + \sigma_{i+1}^{\text{B,A}} + \sigma_i^{\text{B,A}} = 0 \text{ or } 3;$$

$$\Delta n_{\text{solv},i+1}^{\text{A,B}} = -1 \quad \text{otherwise};$$

$$\begin{aligned} P^{\text{A,B}}(i) = & \left[\sum_{i-l}^{i-1} (\sigma_i^{\text{A,B}} - \sigma_i^{\text{B,A}}) + \sum_{i+1}^{i+l} (\sigma_i^{\text{A,B}} - \sigma_i^{\text{B,A}}) - \sigma_i^{\text{B,A}} \right]^2 \\ & - \left[\sum_{i-l}^{i-1} (\sigma_i^{\text{A,B}} - \sigma_i^{\text{B,A}}) \right. \\ & \left. + \sum_{i+1}^{i+l} (\sigma_i^{\text{A,B}} - \sigma_i^{\text{B,A}}) + (1 - \sigma_i^{\text{B,A}}) \right]^2 \end{aligned}$$

where $K_i^{\text{A,B}}$ (meaning K_i^{A} or K_i^{B}) are the equilibrium constants for a line defect at position i on monolayer A or B. The probability of this lattice site to be a line of fluid lipids is then determined $P_f = K/(1 + K)$. A random number, RAN, between zero and one is generated. If $P_f > \text{RAN}$, the lipid is chosen to be in the fluid state, if $P_f < \text{RAN}$, it is chosen to be in the gel state in the next step (see Procedure

in Heimburg and Biltonen, 1996). Because this calculation is designed to be one-dimensional, all m lipids in one line are switched simultaneously. The chain entropy $\Delta S = \Delta H/T_m$ is determined from experimental results (for DPPC: $\Delta H = 8.7$ kcal/mol, $T_m = 314.5$ K).

RESULTS

The above model has been used to calculate heat capacity profiles. Fig. 6 *a* displays the heat capacity profile for a typical set of parameters:

melting enthalpy

$$m \cdot \Delta H = 50 \text{ kcal/mol,}$$

nearest neighbor interaction

$$m \cdot \omega_{\text{gf}} = 1000 \text{ cal/mol,}$$

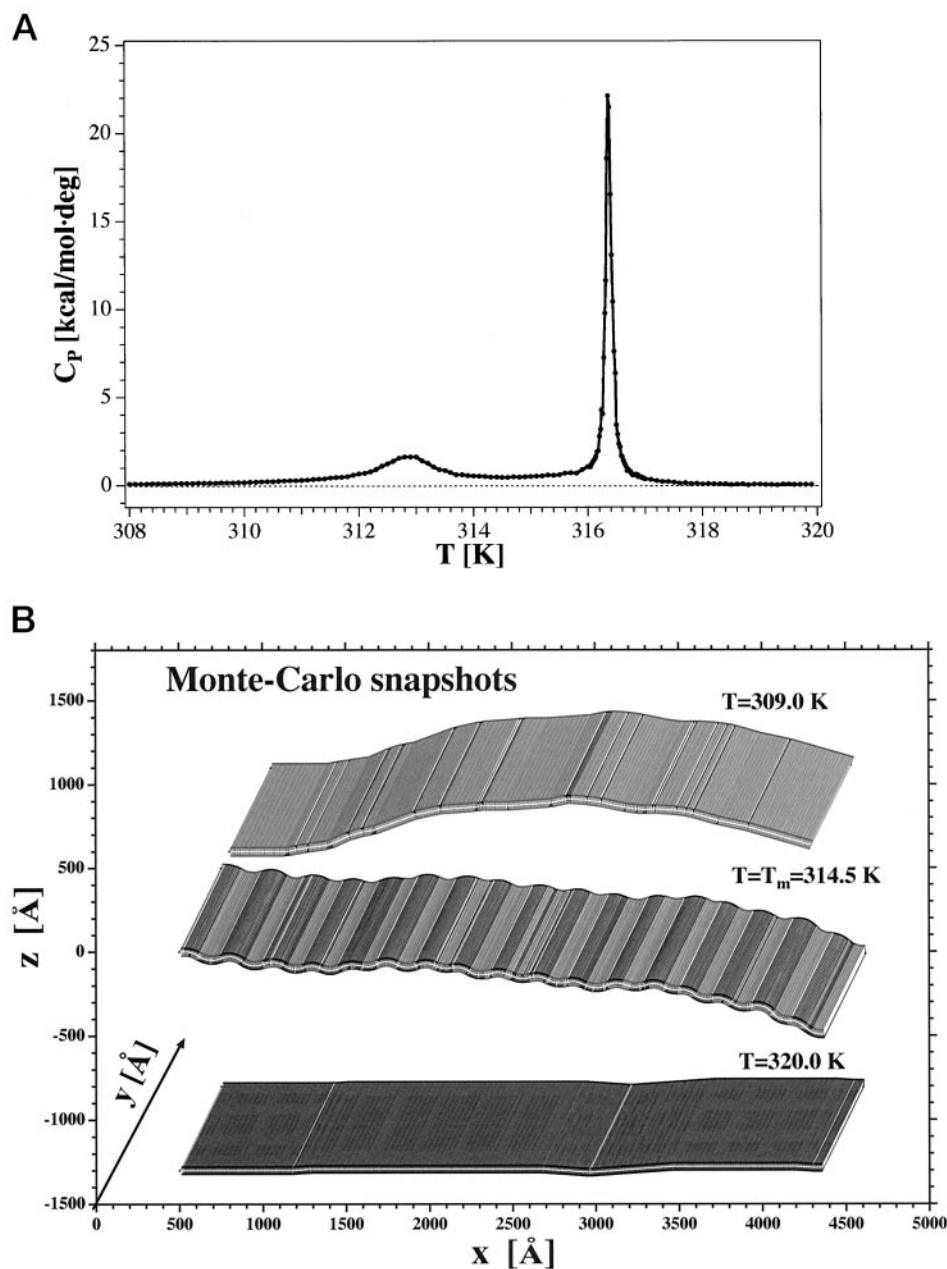
lipid solvent interaction

$$m \cdot \omega_{\text{solv}} = -375 \text{ cal/mol,}$$

ripple period

$$2l + 1 = 41,$$

FIGURE 6 (a) Heat capacity profile of a lipid bilayer in a periodic potential calculated from Monte Carlo simulations using parameters similar to those of DPPC. (b) Representative Monte Carlo snapshots of the simulation presented in the top panel at three different temperatures: 309 K (below the pretransition), 314.5 K (in between pre- and main transition), and 320 K (above the main transition). Parameters are given in the results section.



strength of harmonic potential

$$m \cdot \alpha = 40 \cdot kT = 25 \text{ kcal/mol},$$

where m is the number of lipids per line defect. The computer lattice contained 1000 sites on each monolayer, adopting periodic boundary conditions. Typically, each site was visited 10^4 – 10^6 times during the Monte Carlo procedure. Because DPPC bilayers display a melting enthalpy of ~ 8.7 kcal/mole, the number of lipids in a line defect corresponds to $m \sim 6$. This number, however, should not be taken too seriously, because we neglected finite length effects of the line defects in the model and assumed an all-or-nothing melting along the line defect.

The c_p -profile for the above set of parameters displays two peaks (Fig. 6 *a*). The first maximum is broad and extended, whereas the second maximum is pronounced and cooperative. The heat capacity between the two maxima does not decrease back to the baseline but assumes a higher value, indicating ongoing transition events. In the following, we will assume that the lower peak in the simulation corresponds to the lipid pretransition, whereas the upper peak is the cooperative main transition. In Fig. 6 *b*, three representative Monte Carlo snapshots are given, one below the pretransition, one between pre- and main transition, and one above the main transition. These figures have been constructed from the Monte Carlo lattices assuming an area difference of $\sim 20\%$ between a gel and a fluid lipid, and a membrane thickness in the range of 47 Å. Local interbilayer asymmetries of gel and fluid lipids are assumed to result in a local curvature. The snapshot below the pretransition represents a system where both monolayers are predominantly in the gel state and the membrane is nearly symmetric, and therefore flat. The same is true for the snapshot above the main transition, where both monolayers are predominantly in the fluid lipid state. The snapshot in the intermediate temperature regime, however, displays gel–fluid lipid coexistence, where fluid and gel domains are ordered into a periodic pattern. This pattern is superimposed on the domain structure by the harmonic potential corresponding to the geometric constraints, which were described in the Theory section (Eq. 4). It is quite obvious from this simulation that the change in the membrane geometry, i.e., the formation of membrane ripples, results in a splitting of the chain-melting transition into an extended regime with two maxima at the lower and upper temperature limit. However, this complex behavior is just a consequence of the melting of the lipid chains.

Overall, the model depends on six parameters. The melting enthalpy, ΔH , and the melting temperature, T_m (or $\Delta S = \Delta H/T_m$, respectively) can easily be determined from calorimetric data. The roles of the four other parameters, the potential α , the in-plane cooperativity ω_{gf} , the interaction with solvent ω_{solv} , and the ripple periodicity $2l + 1$, are more indirect. The magnitude of the potential α defines how

strongly confined surface curvature fluctuations are. In Fig. 7 (*top*), theoretical results are given for increasing values of α , corresponding to stronger surface confinement. An increasing value for α leads to a sharpening of both the pre- and the main chain-melting reaction, whereas the splitting between both transitions increases. The simulation results were compared with experimental curves of DPPC vesicles prepared by three different procedures: large unilamellar vesicles prepared by ultrasonication by extrusion, and multilamellar vesicles prepared by dispersion of the lipid in distilled water without further treatment (Fig. 7, *bottom*). These data were adapted from Heimburg (1998). Multilamellar vesicles consist of multilayer stacks that lead to confinement of out-of-plane fluctuations (Helfrich, 1978). Unilamellar vesicles, in contrast, display no bilayer–bilayer interactions, and out-of-plane fluctuations are therefore less confined. In this case, the geometric confinement is smaller, but it does not disappear as long as the membrane maintains a defined shape (for example, a sphere) in which only those curvature fluctuations are allowed that maintain the closed topology. The behavior of the experimental vesicular systems given in Fig. 7 (*bottom*) is very similar to the simulation results. Again, stronger confinement leads to enhanced apparent cooperativity for both the pre- and the main chain-melting transition. Note that, in the center panels of both the calculations (Fig. 7, *top, center*) and the experiments (extruded large unilamellar vesicles, Fig. 7, *bottom, center*), the excess heat capacity is not zero in the temperature interval between pre- and main transition.

Besides the magnitude of the potential α , there are three model parameters that determine the Hamiltonian energy of the membrane states: ω_{gf} , ω_{solv} , and the ripple periodicity $2l + 1$. The effect of the latter three parameters on the heat capacity profiles is demonstrated in Fig. 8. The in-plane interaction parameter, ω_{gf} , will favor the formation of domains of gel or fluid line defects in each monolayer. Its increase leads to a similar result as the increase of the surface confining potential, α . Both the pre- and the main transition become progressively more pronounced (Fig. 8 *a*). The interaction of a curved membrane segment with the aqueous solvent, ω_{solv} , results in an asymmetry of the heat capacity profile. In Fig. 8 *b*, it is shown that, for $\omega_{solv} = 0$, both pre- and main transition display similar areas and cooperativity. Progressively more negative values for ω_{solv} lead to a broadening of the pretransition and an increased cooperativity of the main transition. The location of both transitions on the temperature axis is unaffected. The ripple periodicity, finally, is artificially superimposed on the membrane system by the exact formulation of the surface-confining harmonic potential (Eq. 4). An increase in the ripple periodicity leads to more pronounced pre- and main transition peaks and to an increase of the temperature interval between pre- and main transition (Fig. 8 *c*).

It should be noted that the influences of change in the parameters ω_{gf} , ω_{solv} , ripple periodicity, and α on the heat

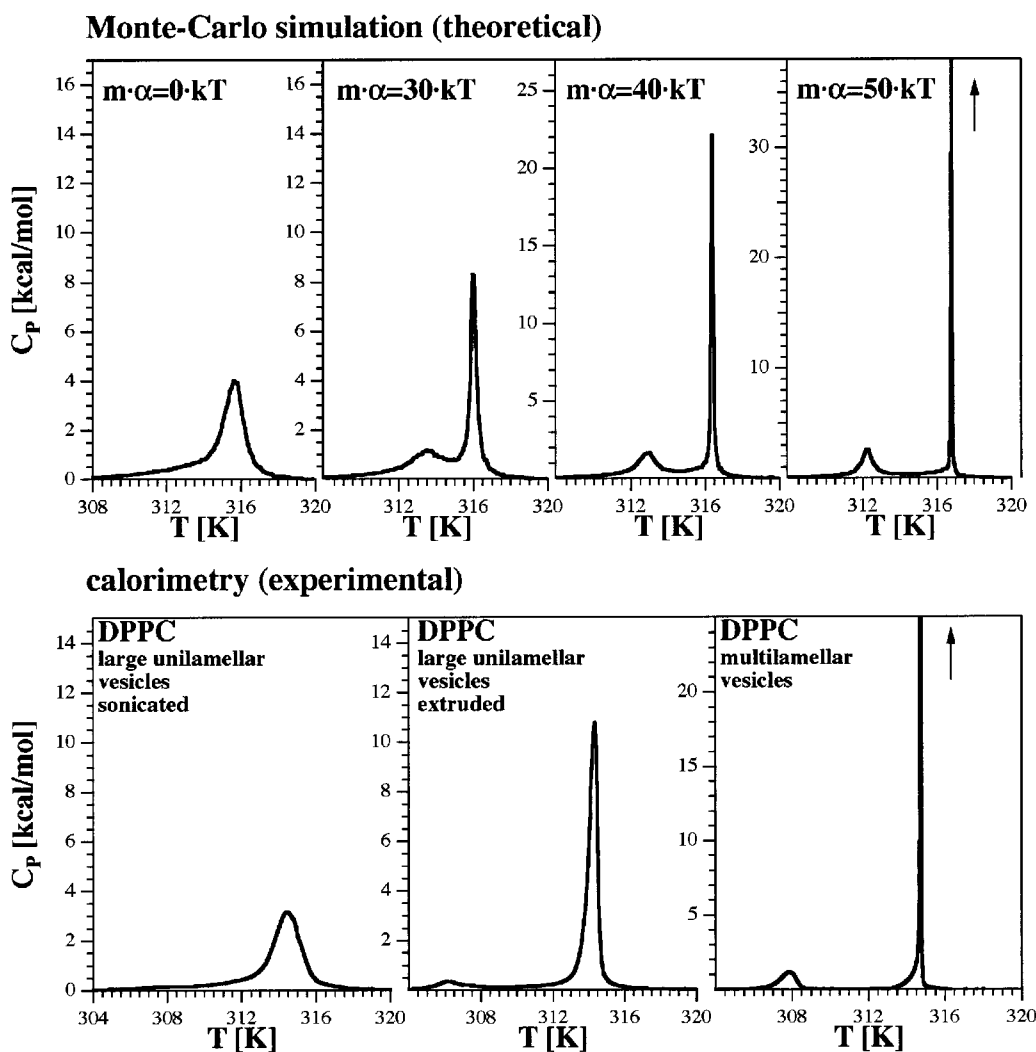


FIGURE 7 Comparing experimental data with simulations. *Top*: Heat capacity profiles at four different values for the harmonic potential amplitude α that depends on structural boundary conditions. Except for the harmonic potential amplitude α , all other parameters are equal to those in Fig. 6 *a*. Upon increasing the potential, both main and pretransition become more pronounced. *Bottom*: Experimental heat capacity data of DPPC vesicles from preparations yielding different vesicular geometries. Sonicated large unilamellar vesicles (*left*), extruded large unilamellar vesicles and multilamellar vesicles (adapted from Heimburg, 1998). The calculations and the experimental data display very similar behavior. Multilamellar stacking corresponds to a large amplitude α for the harmonic potential.

capacity profiles are, in part, counteractive. For example, the in-plane cooperativity, ω_{gf} leads to an increase of the tendency to form large domains of gel or fluid lipid. The ripple period, in contrast, stabilizes the fixed-size domains with half the ripple period in the intermediate temperature regime (Fig. 5).

DISCUSSION

Here, we present a model for the lipid pretransition that is based on the assumption that the pretransition is associated with the chain-melting process. The formation of membrane ripples is assumed to be a consequence of the formation of gel and fluid lipid domains in the individual monolayers,

which, for geometrical and topological reasons, are forced to arrange periodically on the surface. Although the model is simple and the calculation is based on an Ising-like model, it leads to a surprising similarity between calculated heat capacity traces and experimental results. This model is the first to be able to describe the complete heat capacity profile found experimentally. It is distinctly different from other models found in the literature because it considers both pre- and main melting transition as being part of the chain melting. Therefore, in the framework of this model, the pre- and main transition are coupled. The formation of periodic membrane ripples is found to be a consequence of steric intermonolayer interactions and geometric constraints. Thus, an isolated monolayer is predicted not to

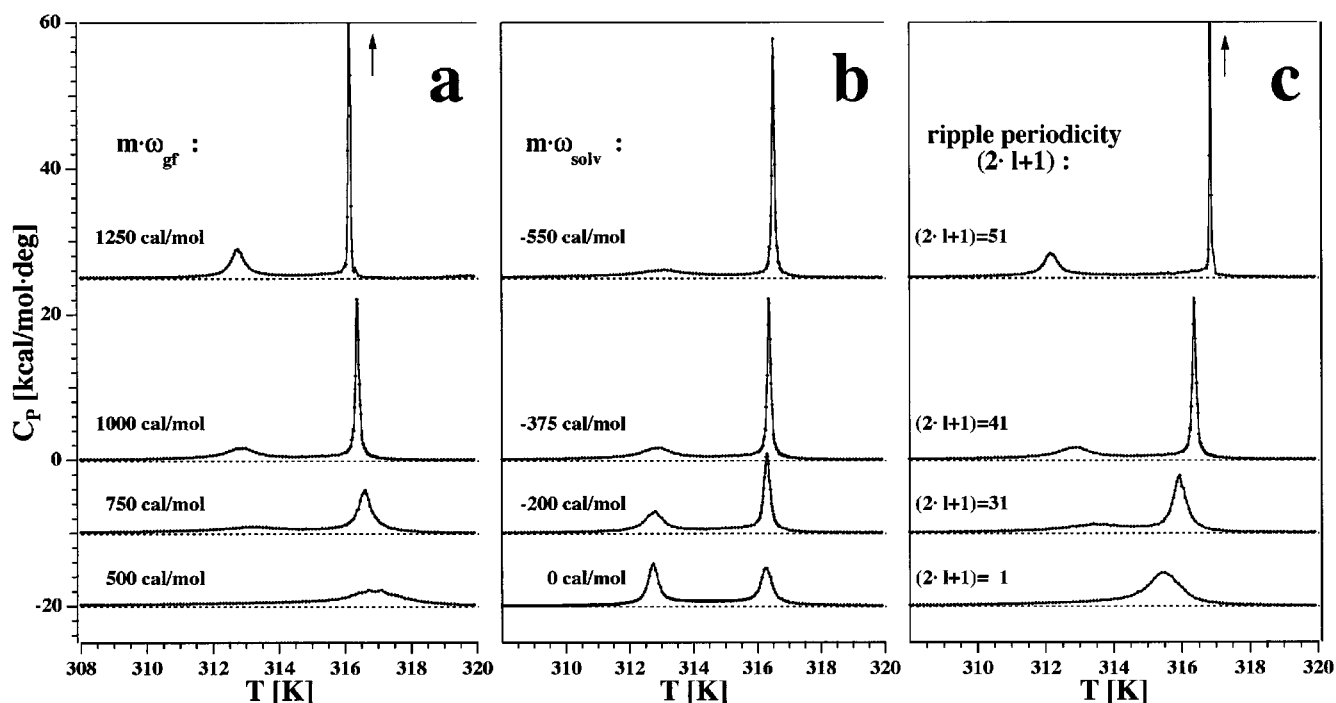


FIGURE 8 Dependence of the membrane melting profile on (a) variation of the in-plane cooperativity parameter, ω_{gf} , (b) variation of the solvent interaction parameter, ω_{solv} , and (c) on the ripple periodicity $2l + 1$. Except for the parameter indicated at each individual c_p -trace, all other parameters are equal to those in Fig. 6 a.

display ripple formation. This may be the reason why ripple formation is not found on a Langmuir trough.

Our model is based on the simplifying assumption that the ripple state originates from the formation of one-dimensional fluid line defects along the principal axis of a triangular lattice. Kato and Kubo (1997) concluded from T-jump experiments that the growth of the ripple edges occurs one-dimensionally along one of the lipid axes, supporting our hypothesis.

The hypothesis that, during the pretransition chain, melting takes place is supported by a large number of experimental observations. First, there is the heat and volume change in both pre- and main chain-melting transition. The ratio of enthalpy and volume changes is on the same order in both transitions (Nagle and Wilkinson, 1978; Heimburg, 1998). This notion is also supported by the finding that pre- and main chain-melting transition temperatures display a similar pressure dependence (Maruyama et al., 1996; Ichimori et al., 1997, 1998). Changes in chain order in the pretransition have been found in ESR measurements (cf. Fig. 1; Tsuchida and Hatta, 1988; Heimburg et al., 1992; Cruz et al., 1998) and in solid-state NMR. Because these methods are sensitive not primarily to changes in static order but rather to changes in the chain mobility, this is a clear indication for a melting process in the pretransition range. In FTIR experiments, the CH-stretching and CH₂-wagging vibrations were monitored, and changes in pretransition and in main transition were found, which are compa-

parable to the changes in enthalpy of the two transition (Le Bihan and Pezolet, 1998). In electron microscopy, it has been found that, in the pretransition, gauche conformers are introduced into the lipid chains (Meyer, 1996). Furthermore, it has been found that the permeability of the lipid membrane for acetic acid displays discontinuous steps both in the pre- and the main chain-melting transition (Xiang and Anderson, 1997). Krasnowska et al. (1998) found that special fluorescent labels, which partition well into the fluid phase but not into the gel phase also partition into the ripple phase, suggesting that this phase has some fluid-like characteristics. One important finding from our simulations is that the excess heat capacity is not zero in between the pre- and the main transition (Fig. 6) as is observed in calorimetric experiments (Fig. 7). This is in agreement with the calorimetric data of Blume (1983), who reported that the excess heat capacity in the *P*₆-phase is ~400 cal/mol·deg higher than in the *L*_a-phase (for DMPC and DPPC multilayers).

The dependence of the two transitions on the model parameters (Figs. 7 and 8) suggest that pre- and main transitions change their cooperativity in a similar manner if one of the parameters is changed. This is clearly a consequence of the prerequisite that they are both consequences of one single physical process. This is in agreement with the observation that unilamellar vesicles display less cooperativity for both transitions as compared to multilamellar vesicles (Fig. 7).

The model contains one parameter that takes care of preferential hydration forces on the ripple phase (Inoko and Mitsui, 1978; Janiak et al., 1979; Doniach, 1979; Parsegian, 1983; Cevc, 1991; Bartucci et al., 1996; Perkins et al., 1997; Krasnowska et al., 1998; Le Bihan and Pezolet, 1998). The origin of these forces may be due to head-group polarity and size. Phosphatidylethanolamines are difficult to disperse in aqueous buffer, and they do not display a pretransition (McIntosh, 1980).

The basic idea of our model is similar to that of an earlier paper by Doniach (1979), who considered ripple formation as the consequence of the competition between head-group ordering favored by elastic forces and a favorable head-group hydration in the ripple state. The present model implicitly takes into account that the curvature fluctuations (and therefore the elasticity) of membranes are high in the transition regime (Hønger et al., 1994; Lemmich et al., 1997; Heimburg, 1998), favoring the formation of the ripple phase.

The model presented here introduces an important concept into the description of chain-melting transitions. Because chain melting is coupled to changes in volume and area, structural changes are superimposed on the transition. Although intermonolayer coupling was introduced in lattice models before (Zhang et al., 1992b), the geometric problems caused by area changes have usually not been taken into account seriously. Hansen et al. (1998) used a mean field approach, which contained similar elements as the model proposed here. It also was designed to couple structural changes to curvature fluctuations, using a potential that confines the global geometry. Papers by Marder et al. (1984) and Leibler and Andelman (1987) follow similar approaches, coupling fluid–gel coexistence with periodic undulations. Those models, however, do not attempt to describe the pretransition in detail or to predict heat capacity profiles.

As long as lipids are arranged on a regular lattice, only a very limited number of gel and fluid lipid arrangements in three-dimensional space are possible, the ripple phase being one of them. If lipids are not arranged on lattices, other geometry changes may be possible. Recently, a transition between lipid vesicles to a bilayer network in the melting regime of DMPG dispersions has been found (Heimburg and Biltonen, 1994; Schneider et al., 1999). Interestingly, in this system, the heat capacity profile also splits into a more complex melting behavior with two pronounced maxima. We claim that this is not by accident. Rather, the coupling of chain melting and a structural change results in a splitting of the melting peak by necessity.

Finally, one should add that, due to the simplicity of our model, it falls short of explaining some details of the ripple phase. The ripple periodicity is a parameter of the calculation and does not automatically drop out of the theory. Rather, it has been chosen to be comparable with experimental results. Because the model contains no tilt axis, it

cannot explain asymmetric ripples. Furthermore, our model may overestimate the overall excess heat of the pretransition, which is usually in the range of 10–20% of the overall excess heat of melting. This is due to the simplifying description of the geometric boundary condition described in Eq. 4. However, in mixtures of DMPC and DMPG, a pretransition has been found that even displays a similar enthalpy to the main transition (Bayerl et al., 1990; cf. Fig. 8 b). In experiments, however, the exact enthalpy of the pretransition is not easily accessible because it depends very sensitively on the exact shape of the baseline over a large temperature interval. It is quite likely that it is usually underestimated.

I am grateful for critical reading and comments by Martin Zuckermann and John H. Ipsen. The predominant part of the model development was done during a visit at the McGill University/Montréal in 1998, where I was a guest of Prof. Zuckermann. This work has been made possible by a grant from the Deutsche Forschungsgemeinschaft (He1829/6–1).

REFERENCES

- Bartucci, R., G. Montesano, and L. Sportelli. 1996. Effects of poly(ethylene glycol) on neutral lipid bilayers. *Colloids Surf. A*. 115:63–71.
- Bayerl, T. M., T. Köchy, and S. Brückner. 1990. On the modulation of a high-enthalpy pretransition in binary mixtures of DMPC and DMPG by polar headgroup interaction. *Biophys. J.* 57:675–680.
- Binder, H., and K. Dittes. 1987. Investigation on the pyrene fluorescence in phospholipid membranes. *Stud. Biophys.* 120:59–71.
- Blume, A. 1983. Apparent molar heat capacities of phospholipids in aqueous dispersion. Effects of chain length and head group structure. *Biochemistry*. 22:5436–5442.
- Bota, A., and M. Kriechbaum. 1998. Prehistory in the pretransition range of dipalmitoyl phosphatidylcholine/water system. *Colloids Surf. A* 141: 441–448.
- Brown, R. E., W. H. Naderson, and V. S. Kulkarni. 1995. Macro-ripple phase formation in bilayers composed of galactosylceramide and phosphatidylcholine. *Biophys. J.* 68:1396–1405.
- Cevc, G. 1991. Polymorphism of the bilayer membranes in the ordered phase and the molecular origin of the lipid pretransition and rippled lamellae. *Biochim. Biophys. Acta*. 1062:59–69.
- Cruz, A., D. Marsh, and J. Perez-Gil. 1998. Rotational dynamics of spin-labelled surfactant-associated proteins SP-B and SP-C in dipalmitoylphosphatidylcholine and dipalmitoylphosphatidylglycerol bilayers. *Biochim. Biophys. Acta*. 1415:125–134.
- Cunningham, B. A., A. D. Brown, D. H. Wolfe, W. P. Williams, and A. Brain. 1998. Ripple phase formation in phosphatidylcholine—effect of acyl chain relative length, position, and unsaturation. *Phys. Rev. E*. 58:3662–3672.
- Czajkowsky, D. M., C. Huang, and Z. Shao. 1995. Ripple phase in asymmetric unilamellar bilayers with saturated and unsaturated phospholipids. *Biochemistry*. 34:12501–12505.
- Doniach, S. 1979. A thermodynamic model for the monoclinic (ripple) phase of hydrated phospholipid bilayers. *J. Chem. Phys.* 70:4587–4596.
- Engelke, M., R. Jessel, A. Wiechmann, and H. A. Diehl. 1997. Effect of inhalation anesthetics on the phase behaviour, permeability and order of phosphatidylcholine bilayers. *Biophys. Chem.* 67:127–138.
- Epps, D. E., C. L. Wilson, A. F. Vosters, and F. J. Kezdy. 1997. The pretransition of dipalmitoyllecithin bilayers as probed by the fluorescent pyrrolopyrimidine, U-104067. *Chem. Phys. Lipids*. 86:121–133.
- Evans, E. A., and R. Kwok. 1982. Mechanical calorimetry of large dimyristoylphosphatidylcholine vesicles in the phase transition region. *Biochemistry*. 21:4874–4879.

- Georgallas, A., and M. J. Zuckermann. 1986. Lipid vertical motion and related steric effects in bilayer membranes. *Eur. Biophys. J.* 14:53–61.
- Hansen, P. L., L. Miao, and J. H. Ipsen. 1998. Fluid lipid bilayers—intermonolayer coupling and its thermodynamic manifestations. *Phys. Rev. E.* 58:2311–2324.
- Heimburg, T. 1998. Mechanical aspects of membrane thermodynamics. Estimation of the mechanical properties of lipid membranes close to the chain melting transition from calorimetry. *Biochim. Biophys. Acta.* 1415:147–162.
- Heimburg, T., and R. L. Biltonen. 1994. The thermotropic behavior of dimyristoyl phosphatidylglycerol and its interaction with cytochrome *c*. *Biochemistry.* 33:9477–9488.
- Heimburg, T., and R. L. Biltonen. 1996. A Monte-Carlo simulation study of protein-induced heat capacity changes and lipid-induced protein clustering. *Biophys. J.* 70:84–96.
- Heimburg, T., U. Würz, and D. Marsh. 1992. Binary phase diagram of hydrated dimyristoyl glycerol-dimyristoyl phosphatidylcholine mixtures. *Biophys. J.* 63:1369–1378.
- Helfrich, W. 1978. Steric interaction of fluid membranes in multilayer systems. *Z. Naturforsch.* 33a:305–315.
- Hinz, H. J., L. Six, K. P. Ruess, and M. Lieflander. 1985. Head-group contributions to bilayer stability: monolayer and calorimetric studies on synthetic, stereochemically uniform glucolipids. *Biochemistry.* 24:806–813.
- Holopainen, J. M., J. Y. A. Lehtonen, and P. K. J. Kinnunen. 1997. Lipid microdomains in dimyristoyl phosphatidylcholine-ceramide liposomes. *Chem. Phys. Lipids.* 88:1–13.
- Hønger, T., K. Mortensen, J. H. Ipsen, J. Lemmich, R. Bauer, and O. G. Mouritsen. 1994. Anomalous swelling of multilamellar lipid bilayers in the transition region by renormalization of curvature elasticity. *Phys. Rev. Lett.* 72:3911–3914.
- Hui, S. W., R. Viswanathan, J. A. Zasadzinski, and J. N. Israelachvili. 1995. The structure and stability of phospholipid bilayers by atomic force microscopy. *Biophys. J.* 68:171–178.
- Ichimori, H., T. Hata, H. Matsuki, and S. Kaneshina. 1998. Barotropic phase transitions and pressure-induced interdigitation on bilayer membranes of phospholipids with varying acyl chain lengths. *Biochim. Biophys. Acta.* 1414:165–174.
- Ichimori, H., T. Hata, T. Yoshioka, H. Matsuki, and S. Kaneshina. 1997. Thermotropic and barotropic phase transition on bilayer membranes of phospholipids with varying acyl chain-lengths. *Chem. Phys. Lipids.* 89:97–105.
- Inoko, Y., and T. Mitsui. 1978. Structural parameters of dipalmitoyl phosphatidylcholine lamellar phases and bilayer phase transitions. *J. Phys. Soc. Japan.* 44:1918–1924.
- Janiak, M. J., D. M. Small, and G. G. Shipley. 1976. Nature of the thermal pretransition of synthetic phospholipids: dimyristoyl- and dipalmitoyl- lecithin. *Biochemistry.* 15:4575–4580.
- Janiak, M. J., D. M. Small, and G. G. Shipley. 1979. Temperature and compositional dependence of the structure of hydrated dimyristoyl lecithin. *J. Biol. Chem.* 254:6068–6078.
- Jørgensen, K. 1995. Calorimetric detection of a sub-main transition in long-chain phosphatidylcholine lipid bilayers. *Biochim. Biophys. Acta.* 1240:111–114.
- Kato, S., and T. Kubo. 1997. Relaxation process after the cooling jump across the pretransition of dipalmitoyl phosphatidylcholine bilayers. *Chem. Phys. Lipids.* 90:31–44.
- Kodama, M., and T. Miyata. 1996. Effect of the head group of phospholipids on the acyl-chain packing and structure of their assemblies as revealed by microcalorimetry and electron microscopy. *Colloids Surf. A.* 109:283–289.
- Koiv, A., P. Mustonen, and P. K. Kinnunen. 1993. Influence of sphingosine on the thermal phase behaviour of neutral and acidic phospholipid liposomes. *Chem. Phys. Lipids.* 66:123–134.
- Krasnowska, E. K., Gratton, E., and T. Parasassi. 1998. Prodan as a membrane surface fluorescence probe—partitioning between water and phospholipid phases. *Biophys. J.* 74:1984–1993.
- Le Bihan, T., and M. Pezolet. 1998. Study of the structure and phase behavior of dipalmitoyl phosphatidylcholine by infrared spectroscopy—characterization of the pretransition and subtransition. *Chem. Phys. Lipids.* 94:13–33.
- Leibler, S., and D. Andelman. 1987. Ordered and curved meso-structures in membranes and amphiphilic films. *J. Physique.* 48:2013–2018.
- Lemmich, J., K. Mortensen, J. H. Ipsen, T. Honger, R. Bauer, and O. G. Mouritsen. 1997. The effect of cholesterol in small amounts on lipid bilayer softness in the region of the main phase transition. *Eur. Biophys. J.* 25:293–304.
- Lentz, B. R., E. Freire, and R. L. Biltonen. 1978. Fluorescence and calorimetric studies of phase transitions in phosphatidylcholine multilayers: kinetics of the pretransition. *Biochemistry.* 17:4475–4480.
- Lichtenberg, D., M. Menashe, S. Donaldson, and R. L. Biltonen. 1984. Thermodynamic characterization of the pretransition of unilamellar dipalmitoyl-phosphatidylcholine vesicles. *Lipids.* 19:395–400.
- Lubensky, T. C., and F. C. MacKintosh. 1993. Theory of “ripple” phases of lipid bilayers. *Phys. Rev. Lett.* 71:1565–1568.
- Marder, M., H. L. Frisch, J. S. Langer, and H. M. McConnell. 1984. Theory of the intermediate rippled phase of phospholipid bilayers. *Proc. Natl. Acad. Sci. USA.* 81:6559–6561.
- Maruyama, S., H. Matsuki, H. Ichimori, and S. Kaneshina. 1996. Thermotropic and barotropic phase behavior of dihexadecyl phosphatidylcholine bilayer membrane. *Chem. Phys. Lipids.* 82:125–132.
- Matuoka, S., S. Kato, and I. Hatta. 1994. Temperature change of the ripple structure in fully hydrated dimyristoyl phosphatidylcholine/cholesterol multibilayers. *Biophys. J.* 67:728–736.
- Mavromoustakos, T., E. Theodoropoulou, and D. P. Yang. 1997. The use of high-resolution solid-state NMR spectroscopy and differential scanning calorimetry to study interactions of anesthetic steroids with membrane. *Biochim. Biophys. Acta.* 1328:65–73.
- Mavromoustakos, T., E. Theodoropoulou, D. Papahatjis, T. Kourouli, D. P. Yang, M. Trumbore, and A. Makriyannis. 1996. Studies on the thermotropic effects of cannabinoids on phosphatidylcholine bilayers using differential scanning calorimetry and small angle x-ray diffraction. *Biochim. Biophys. Acta.* 1281:235–244.
- McCullough, W. S., and H. L. Scott. 1990. Statistical-mechanical theory of the ripple phase of lipid bilayers. *Phys. Rev. Lett.* 65:931–934.
- McIntosh, T. J. 1980. Differences in hydrocarbon chain tilt between hydrated phosphatidylethanolamine and phosphatidylcholine bilayers. A molecular packing model. *Biophys. J.* 29:237–245.
- Metropolis, N., A. W. Rosenbluth, M. N. Rosenbluth, A. H. Teller, and E. Teller. 1953. Equations of state calculations by fast computing machines. *J. Chem. Phys.* 21:1087–1092.
- Meyer, H. W. 1996. Pretransition-ripples in bilayers of dipalmitoyl phosphatidyl choline-undulation or periodic segments—a freeze-fracture study. *Biochim. Biophys. Acta.* 1302:138–144.
- Meyer, H. W., B. Dobner, and K. Semmler. 1996. Macroripple-structures induced by different branched-chain phosphatidylcholines in bilayers of dipalmitoyl phosphatidyl choline. *Chem. Phys. Lipids.* 82:179–189.
- Mortensen, K., W. Pfeiffer, E. Sackmann, and W. Knoll. 1988. Structural properties of a phosphatidylcholine-cholesterol system as studied by small-angle neutron scattering: ripple structure and phase diagram. *Biochim. Biophys. Acta.* 945:221–245.
- Nagle, J. F., and D. A. Wilkinson. 1978. Lecithin bilayers—density measurements and molecular interactions. *Biophys. J.* 23:159–175.
- Parsegian, V. A. 1983. Dimensions of the “intermediate” phase of dipalmitoyl phosphatidylcholine. *Biophys. J.* 44:413–415.
- Perkins, W. R., X. G. Li, J. L. Slater, P. A. Harmon, P. L. Ahl, S. R. Minchey, S. M. Gruner, and A. S. Janoff. 1997. Solute-induced shift of phase transition temperature in di-saturated PC liposomes—adoption of ripple phase creates osmotic stress. *Biochim. Biophys. Acta.* 1327:41–51.
- Pink, D. A., T. J. Green, and D. Chapman. 1980. Raman scattering in bilayers of saturated phosphatidylcholines. *Exp. Theor. Biochem.* 19:349–356.
- Prenner, E. J., R. N. A. H. Lewis, L. H. Kondejewski, R. S. Hodges, and R. N. McElhaney. 1999. Differential scanning calorimetric study of the effect of the antimicrobial peptide gramicidin S on the thermotropic

- phase behavior of phosphatidylcholine, phosphatidylethanolamine and phosphatidylglycerol lipid bilayer membranes. *Biochim. Biophys. Acta.* 1417:211–223.
- Rand, R. P., D. Chapman, and K. Larsson. 1975. Tilted hydrocarbon chains of dipalmitoyl lecithin become perpendicular to the bilayer before melting. *Biophys. J.* 15:1117–1124.
- Rappolt, M., and G. Rapp. 1996. Structure of the stable and metastable ripple phase of dipalmitoylphosphatidylcholine. *Eur. Biophys. J.* 24: 381–386.
- Sackmann, E. 1995. Physical basis of self-organization and function of membranes: physics of vesicles. In *Structure and Dynamics of Membranes: From Cells to Vesicles*. R. Lipowski and E. Sackmann (eds.), Elsevier, Amsterdam, The Netherlands. 213–304.
- Schneider, M. F., W. Jahn, D. Marsh, B. Kloesgen, and T. Heimburg. 1999. Network formation of lipid membranes—triggering structural transitions by chain melting. *Proc. Natl. Acad. Sci. USA.* 96:14312–14317.
- Scott, H. L., and P. A. Pearce. 1989. Calculation of intermolecular interaction strengths in the $P\beta$ in lipid bilayers. Implications for theoretical models. *Biophys. J.* 55:339–345.
- Scott, H. L., and W. S. McCullough. 1991. Theories of the modulated 'ripple' phase of lipid bilayers. *Int. J. Mod. Phys. B.* 5:2479–2497.
- Scott, H. L., and W. S. McCullough. 1993. Lipid-cholesterol interactions in the $P\beta$ phase: application of a statistical mechanical model. *Biophys. J.* 64:1398–1404.
- Sugar, I. P., R. L. Biltonen, and N. Mitchard. 1994. Monte Carlo simulations of membranes: phase transition of small unilamellar dipalmitoylphosphatidylcholine vesicles. *Meth. Enzymol.* 240:569–593.
- Suurkuusk, Y., B. T. Lentz, Y. Barenholtz, R. L. Biltonen, and T. E. Thompson. 1976. Calorimetric and fluorescent-probe study of the gel–liquid crystalline phase-transition in small, single-lamellar dipalmitoylphosphatidylcholine vesicles. *Biochemistry.* 15:1393–1401.
- Tomoaia-Cotisel, M., and I. W. Levin. 1997. Thermodynamic study of the effects of ursodeoxycholic acid and ursodeoxycholate on aqueous dipalmitoyl phosphatidylcholine bilayer dispersions. *J. Phys. Chem. B.* 101:8477–8485.
- Tsuchida, K., and I. Hatta. 1988. ESR studies on the ripple phase in multilamellar phospholipid bilayers. *Biochim. Biophys. Acta.* 945: 73–80.
- Woodward, J. T. IV, and J. A. Zasadzinski. 1996. Amplitude, wave form, and temperature dependence of bilayer ripples in the $P\beta$ phase. *Phys. Rev. E.* 53:R3044–R3047.
- Xiang, T. X., and B. D. Anderson. 1997. Permeability of acetic acid across gel and liquid–crystalline lipid bilayers conforms to free-surface-area theory. *Biophys. J.* 72:223–237.
- Zhang, Z., M. Laradji, H. Guo, O. G. Mouritsen, and M. J. Zuckermann. 1992a. Phase behavior of pure lipid bilayers with mismatch interactions. *Phys. Rev. A* 45:7560–7567.
- Zhang, Z., M. M. Sperotto, M. J. Zuckermann, and O. G. Mouritsen. 1993. A microscopic model for lipid/protein bilayers with critical mixing. *Biochim. Biophys. Acta.* 1147:154–160.
- Zhang, Z., M. J. Zuckermann, and O. G. Mouritsen. 1992b. Effect of intermonolayer coupling on the phase behavior of lipid bilayers. *Phys. Rev. A* 46:6707–6713.